Comparative Analysis of Edge- and Broadside-Coupled Split Ring Resonators for Metamaterial Design—Theory and Experiments

Ricardo Marqués, *Member, IEEE*, Francisco Mesa, *Member, IEEE*, Jesús Martel, and Francisco Medina, *Senior Member, IEEE*

***Abstract*—This paper develops a quasi-analytical and self-consistent model to compute the polarizabilities of split ring resonators (SRRs). An experimental setup is also proposed for measuring the magnetic polarizability of these structures. Experimental data are provided and compared with theoretical results computed following the proposed model. By using a local field approach, the model is applied to the obtaining of the dispersion characteristics of discrete negative magnetic permeability and left-handed metamaterials. Two types of SRRs, namely, the so-called edge coupled- and broadside coupled- SRRs, have been considered. A comparative analysis of these two structures has been carried out in connection with their suitability for the design of metamaterials. Advantages and disadvantages of both structures are discussed.**

***Index Terms*—Left-handed media (LHM), metamaterials, negative magnetic permeability, negative refractive index, split ring resonators (SRRs).**

I. Introduction

THE term *metamaterial* is presently applied to artificial discrete media showing "exotic" electromagnetic properties at microwave frequencies. These media include artificial plasmas [1]–[3] (which exhibits negative dielectric permittivity below their plasma frequency), negative magnetic permeability media (NMPM) [4] and left-handed media (LHM) [5], [6] (these are media with simultaneously negative electric permittivity and magnetic permeability). Artificial plasmas are well-known materials that can be built up, for instance, by using a regular array or mesh of wires and/or metallic plates [1]. The electromagnetic behavior of these wire/plate-made artificial plasmas is well understood, their electromagnetic models leading to accurate predictions in most cases [1]–[3]. In practice, an artificial NMPM has been recently demonstrated making use of small resonant particles , the so-called split ring resonators (SRRs) introduced in [4], arranged in a convenient way. Discrete LHM, in turn, have been developed by combining an artificial NMPM with an artificial plasma working below its plasma frequency [6]–[9].

Up to date, most of the electromagnetic analysis of NMPM and LHM have involved electromagnetic full-wave simulations [6], [10], [11]. However, as far as these media are expected to be properly described by a continuous-medium approach, the dimensions of their unit cell should be a small fraction of the free space wavelength (otherwise the incident waves would be diffracted rather than refracted by the metamaterial). This suggests and allows for the use of an alternative treatment starting from the analysis of the polarizabilities of the elementary constituents of the metamaterial followed by an appropriate homogenization procedure [12]. This local field approach has been succesfully applied in the past to the analysis of artificial dielectrics [13], artificial diamagnetics [14], [15], artificial chiral media [16]–[18] and artificial bianisotropic media [19]. This *local field* approach has other advantages over the full-wave simulations than the obvious simplicity. First of all, it may provide an additional physical insight on the electromagnetic behavior of the medium, which cannot be easily extracted from the rather *blind* numerical simulations. On the other hand, it is expected that the convenient size reduction in the discrete components and unit cells employed in the design of new metamaterials makes the full-wave simulation more and more involved or unappropriate whereas the aforementioned *local field* theories would become more and more accurate.

A local field approach for the analysis of LHM and NMPM implies a model for the behavior of the constituent particles in a quasiuniform incident field. In [20] some of the authors presented a first approach to such analysis for the SRRs [4], which made it possible to detect cross polarization effects in the edge-coupled SRR (EC-SRR) particle proposed by Pendry [4]. A modified SRR particle was proposed in [20] to avoid the above bianisotropy. Since the rings are broadside-coupled in this latter particle, it will be called in the following broadside-coupled SRR (BC-SRR). The feasibility of this new particle for the design of two-dimensional isotropic LHM was numerically and experimentally shown in [9]. Nevertheless, the physical models underlying the aforementioned computations have never been presented in a closed and self-consisten way, nor properly validated by direct measurements of the main properties of both particles.

In this way, the present paper will present a complete and metamaterial design-oriented model for both the EC- and BC-SRRs, together with a proper experimental validation of

Manuscript received July 26, 2002; revised February 4, 2003. This work was supported by the Spanish Ministry of Science and Technology and FEDER funds (Project TIC2001-3163).

R. Marqués and F. Medina are with the Grupo de Microondas, Department of Electrónica & Electromagnetismo, Facultad de Física, Universidad de Sevilla, 41012 Seville, Spain (e-mail: marques@us.es, medina@us.es).

F. Mesa is with the Grupo de Microondas, Department of Física Aplicada 1, E.T.S. de Ingeniería Informática, Universidad de Sevilla, 41012 Seville, Spain (e-mail: mesa@us.es).

J. Martel is with the Grupo de Microondas, Department of Física Aplicada 2, E.T.S. de Arquitectura, Universidad de Sevilla, 41012 Seville, Spain (e-mail: martel@us.es).

Digital Object Identifier 10.1109/TAP.2003.817562

the model. Further, the advantages and disadvantages of both types of particles will be discussed. The paper is organized as follows: Section II thoroughly develops the proposed model for the EC-SRR and the BC-SRR. The analysis in this section follows and completes the previous analysis in [20] and [9], which results in a self-consistent and quasi-analytical method for computing the frequency of resonance and the polarizabilities of the analyzed particles. Next, Section III presents a new method to obtain experimentally the above parameters. Specifically, the proposed method provides the frequency of resonance and the magnetic polarizability of the SRRs, which are the most relevant parameters for metamaterial design. In Section IV, the theoretical results are compared with our experimental data and previously published results. Once the model has been successfully validated by the above comparisons, it is used to evaluate the potential of both EC-SRRs and BC-SRRs for metamaterial design.

II. Theory

This section will describe the models for the polarizabilities of both types of SRRs and for the composite NMPM and LHM metamaterials based on those particles. The EC-SRR and BC-SRR to be analyzed are shown in Fig. 1(a) and (b). In both cases two similar split rings are coupled by means of a strong distributed capacitance in the region between the rings (the slits are meaningfully wider than the distance between the rings, d and t, respectively). When a time-harmonic *external* (or *local*) magnetic field of angular frequency ω is applied along the z axis of these structures, an electromotive force will appear around the SRRs. Provided that the electrical size of the SRR can be considered small, a quasistatic behavior is expected. With this quasistatic model in mind, it is not difficult to see how the induced current lines will pass from one ring to the other through the capacitive gaps between them in the form of field displacement current lines (the current lines can be viewed as tracing almost circular trips). Therefore, the total current intensity flowing on both rings remains the same for any cross section of the structure (i.e., it is independent of the angular polar coordinate). The whole device then behaves as an LC circuit driven by an external electromotive force. The total capacitance of this LC circuit will be the series capacitance of the upper and the lower halves (with respect the line containing the ring gaps) of the SRR and the resonance frequency ω_0 is given by

$$\omega_0 = \sqrt{\frac{2}{\pi r_0 L C_{\text{pul}}}} \tag{1}$$

where C_{pul} is the per unit length (p.u.l.) capacitance between the rings, L is the total inductance of the SRR, and r_0 is the average radius of the considered SRR.

The above result for the resonance frequency (1) is confirmed by a more detailed electromagnetic analysis [20] that also provides the polarizabilities as a function of L, C_{pul} and other geometrical and constitutive parameters of the EC-SRR. This analysis can be extended to the BC-SRR by simply neglecting the

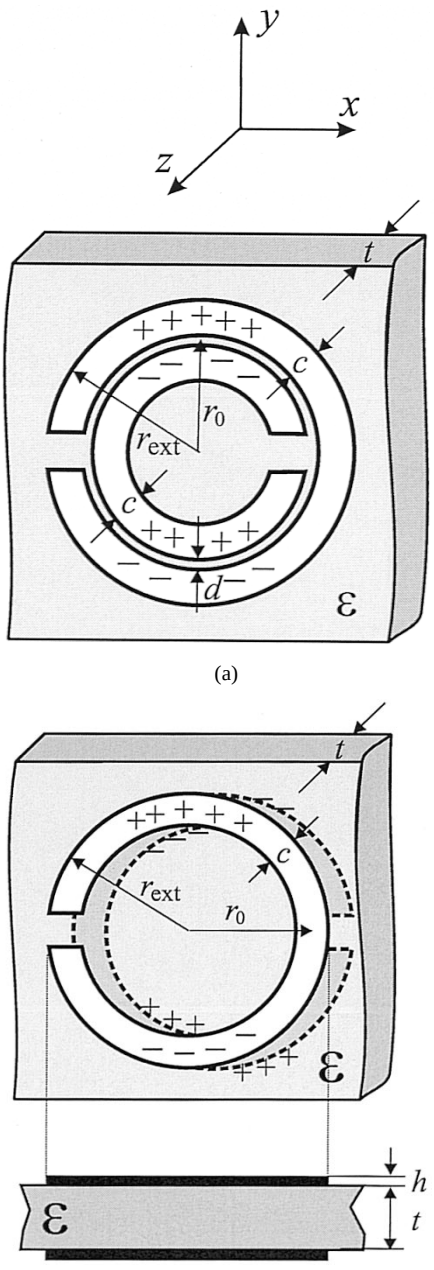

Fig. 1. Two types of SRR. (a) Edge coupled SRR (EC-SRR). (b) Broadside coupled SRR (BC-SRR).

cross-polarization effects that were present in the EC-SRR particle [20]. The resulting equations can be summarized as follows:

- For the EC-SRR:

$$m_z = \alpha_{zz}^{mm} B_z^{\text{ext}} - j\alpha_{yz}^{em} E_y^{\text{ext}} \tag{2}$$

$$p_y = (\alpha_{yy}^{ee} + \alpha_{yy}^{\prime ee}) E_y^{\text{ext}} + j\alpha_{yz}^{em} B_z^{\text{ext}} \tag{3}$$

$$p_x = \alpha_{xx}^{ee} E_x^{\text{ext}} \tag{4}$$

- For the BCSRR:

$$m_z = \alpha_{zz}^{mm} B_z^{\text{ext}} \tag{5}$$

$$p_y = \alpha_{yy}^{ee} E_y^{\text{ext}} \tag{6}$$

$$p_x = \alpha_{xx}^{ee} E_x^{\text{ext}} \tag{7}$$

where m and p are the magnetic and electric induced dipoles, $\mathbf{B}^{\text{ext}}$ and $\mathbf{E}^{\text{ext}}$ the external fields and α the polarizabilities, which are found to be [20]

$$\alpha_{zz}^{mm} = \alpha_0 \left(\frac{\omega_0^2}{\omega^2} - 1 \right)^{-1} \quad , \quad \alpha_0 = \frac{\pi^2 r_0^4}{L} \tag{8}$$

$$\alpha_{xx}^{ee} = \alpha_{yy}^{ee} = \varepsilon_0 \frac{16}{3} r_{\text{ext}}^2 \tag{9}$$

$$\alpha_{yz}^{em} = 2\omega_0 \pi r_0^2 d_{\text{eff}} C_{0,\text{pul}} \frac{\omega}{\omega_0} \left(\frac{\omega_0^2}{\omega^2} - 1 \right)^{-1} \tag{10}$$

$$\alpha_{yy}'^{ee} = 4\omega_0^2 r_0^2 d_{\text{eff}}^2 C_{0,\text{pul}}^2 L \left(\frac{\omega_0^2}{\omega^2} - 1 \right)^{-1} \tag{11}$$

with $d_{\text{eff}} = c + d$ and $C_{0,\text{pul}}$ being the p.u.l. capacitance between the rings when the dielectric slab is removed. In (5)–(11) subscripts stand for cartesian components and superscripts for magnetic/magnetic (mm), electric/electric (ee) or electric/magnetic (em) interaction between the particle and the external field.

Ohmic losses can be approximately incorporated to the model by means of an effective resistance of the rings R that can be introduced as an imaginary part of the total inductance L thus, giving the following complex inductance:

$$\hat{L} = L + \frac{R}{j\omega} \tag{12}$$

which substitutes to L in the above expressions for the polarizabilities.

The computation of the SRR polarizabilities using the above expressions requires the evaluation of L, C_{pul} and $C_{0,\text{pul}}$. Assuming that the ring curvature has negligible effect, a large number of methods for computing the p.u.l. capacitance between the rings of both the EC-SRR and the BC-SRR can be found in the literature (see, for instance, [21] and references therein). For the present purposes it has been found that the closed expressions given in [21, Tables 2.6 and 2.7] give enough accuracy. These tables provide design formulas for the phase constant β and the impedance Z of a *microstrip* transmission line and a pair of coupled metallic strips on a dielectric substrate, respectively. The p.u.l. capacitance, C_{pul}, of these structures are obtained from the well-known expression: $C_{\text{pul}} = \beta/(\omega Z)$ [21]. Once they are obtained, the p.u.l. capacitance of the pair of coupled strips directly gives the C_{pul} of the EC-SRR. For the BC-SRR it can be observed that the p.u.l. capacitance of a pair of coupled metallic strips separated by a dielectric sheet of thickness t [see Fig. 1(b)] is half the p.u.l. capacitance of a single microstrip transmission line on a sheet made of the same dielectric and thickness $t/2$, which can be obtained from the formulas in [21, Table 2.6]. The proposed method of computation is fast and, as was aforementioned, gives enough accuracy in the frame of the present model. However, better results could be obtained by using more specific methods which can take into account the effects of curvature (see [22] for a deeper discussion on this topic). Nevertheless, this improvement only would have sense if other aspects of the model, such as the computation of the ring inductance, are improved too.

The computation of the total inductance L of the SRRs is not so straightforward, although an appropriate approximation can provide a considerable simplification while keeping reasonable accuracy. According to the previous assumptions on the behavior of the line currents along the SRRs, it can be assumed that the total inductance of both SRRs can be approximated by the inductance of a *single* equivalent ring whose average radius is the average radius of the considered SRR and width equal to the width c of each original ring (see Fig. 2). The inductance can be then computed making use of the variational expression $L = 2U_M/I^2$, where U_M is the magnetostatic energy for the total current intensity I supported by the ring. Solving for the magnetostatic potential in the Fourier-Bessel domain, and after some algebraic manipulations, it is finally obtained that (see Appendix)

$$L = \frac{\mu_0 \pi^2}{I^2} \int_0^\infty [\tilde{I}(k)]^2 k^2 \, dk \tag{13}$$

where $\tilde{I}(k)$ is the Fourier-Bessel transform of the *current function* on the ring, $I(r)$ defined by

$$I(r) = \int_r^\infty J_{s,\phi}(r') \, dr' \tag{14}$$

with $J_{s,\phi}$ being the azimuthal surface current density on the ring. For practical computations it has been assumed a constant value for $J_{s,\phi}$ on the ring, that is,

$$J_{s,\phi} = \begin{cases} \frac{I}{c} & \text{for } r_0 - \frac{c}{2} < r < r_0 + \frac{c}{2} \\ 0 & \text{otherwise.} \end{cases} \tag{15}$$

This approximation, taking into account the variational nature of (13), gives a reasonable approximation for L. In this case, the Fourier-Bessel transform, $\tilde{I}(k)$, is analytically obtained in terms of the Struve and Bessel functions (see Appendix) and the integration in (13) is carried out numerically. A better approximation could be obtained if a more accurate description for $J_{s,\phi}$ (multiple basis functions) had been employed. Nevertheless, this numerical improvement is not expected to enhance substantially the quality of the approach since other approximations are already involved in the theory.

Finally, as aforementioned, ohmic losses are introduced in the model by means of the effective resistance, R, of the SRR. This effective resistance is obtained by using the equivalent ring model for the current distribution on the SRR. If a constant $J_{s,\phi}$ is assumed on the ring of Fig. 2, the resistance can be approximated as

$$R = \begin{cases} \frac{2\pi r_0}{ch\sigma}, & \text{if } \frac{h}{2} < \delta \\ \frac{\pi r_0}{c\delta\sigma}, & \text{otherwise} \end{cases} \tag{16}$$

where δ is the skin depth and h and σ the thickness and conductivity of the metallization, respectively.

Once the EC-SRR and the BC-SRR polarizabilities have been obtained in a self-consistent way, they can be used in a local field theory in order to determine the *macroscopic* constitutive parameters of media consisting of a regular array of SRRs. This local field theory makes use of the well-known Lorentz theory [13], [12] and directly applies to any SRR-based NMPM. It can be also applied to the analysis of discrete LHM made by the superposition of an artificial plasma and a SRR-based NMPM. In this latter application, it will be implicitly assumed that the constitutive parameters of the LHM media are the superposition of those of the artificial plasma and the NMPM. Although

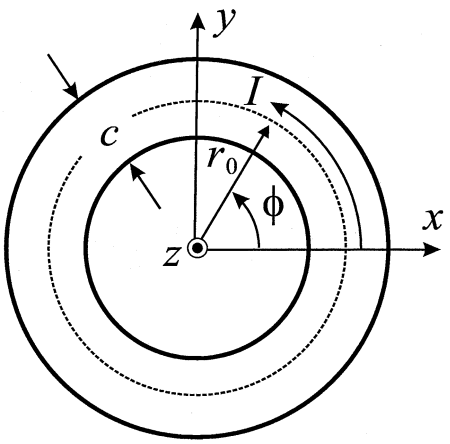

Fig. 2. Equivalent single ring model for computing L of both SRRs. In both cases c is the width of the original rings and r_0 the average radius of the whole structure (see also Fig. 1).

this assumption is not always justified (the general conditions for the validity of this assumption are discussed in [23]), it has been found to be in good agreement with experimental results [6]–[9] and numerical simulations [6], [10], [11]. Subjected to this restriction, the application of the proposed theory to discrete LHM would account for the artificial plasma by simply introducing an additional effective dielectric susceptibility, χ_{eff} (which may be tensorial for anisotropic artificial plasmas). For a 2-D artificial plasma made of a regular array of parallel metallic plates separated a distance a, and for electric field polarization and wave propagation both parallel to the plates, χ_{eff} is given by [1]

$$\chi_{\text{eff}} = -\left(\frac{\omega_0}{\omega}\right)^2 \tag{17}$$

where ω_0 plays the role of an effective *plasma frequency*, which coincides with the cutoff frequency of the parallel-plate waveguides: $\omega_0 = \pi(a\sqrt{\varepsilon_0\mu_0})^{-1}$. For 2- and 3-D arrays of wires, the expressions for χ_{eff} and ω_0 may become more complicated [1], [3], [4].

III. Experimental Setup

At the frequencies of interest for metamaterial design (i.e., near the first resonance) the dominant effect in both the EC-SRR and BC-SRR particles turns out to be the magnetic polarizability accounted for by the α_{zz}^{mm} parameter. This polarizability gives rise to a strong diamagnetic behavior near and above resonance [4], [20], thus playing an essential role in the design of NMPM and LHM. Another relevant effect in the EC-SRR particle is cross-polarization, which results in a bianisotropic behavior of those NMPM and LHM designed using this particle. Since the experimental evidence of this latter effect has been already discussed [20], this section will focus specifically on the experimental determination of the magnetic polarizability of the EC-SRR and BC-SRR (this latter particle does not exhibit magnetoelectric coupling). According to (8), the main parameters to be determined are the resonance frequency, ω_0, and the nonresonant factor α_0.

A simple way of determining the resonance frequency consists in placing the resonator in a hollow waveguide at a location where the electromagnetic field could excite it and to measure the *dip* in the transmission coefficient (or, alternatively, the *peak* in the reflection coefficient) [24]. In fact, this method only provides the resonance frequency of an infinite array of periodically repeated particles, which is shifted over the resonance frequency of a single particle. However, if the dimensions of the waveguide cross section are several times those of the SRR, this shift is not very important [24]. This technique, however, does not provide any information about α_0. In order to obtain a measure of α_0, the experimental setup has been modified in the way shown in Fig. 3. The SRR is placed inside a small circular aperture practiced in a metallic screen located in the middle of the rectangular waveguide. The input and the output are two commercial coaxial to rectangular waveguide transitions. When the $|S_{21}|$ for this structure is measured, typical plots as that shown in Fig. 4 are obtained. The *peak* corresponds to the resonance frequency (1), for which the magnetic dipole of the particle becomes a maximum. The *dip* in the $|S_{21}|$ can be explained by using Bethe's theory of diffraction through small apertures [25], [26]. Following this theory, the aperture without the SRR will radiate toward the output as an equivalent magnetic dipole of strength

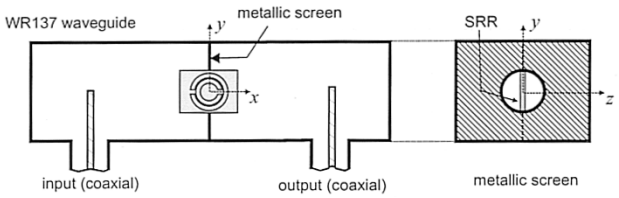

Fig. 3. Scheme of the experimental setup for measuring the SRRs magnetic polarizabilities. The SRR is placed inside a circular aperture made in a metallic screen placed in the rectangular waveguide. For the reported experiments the diameter of the aperture was $R = 6$ mm.

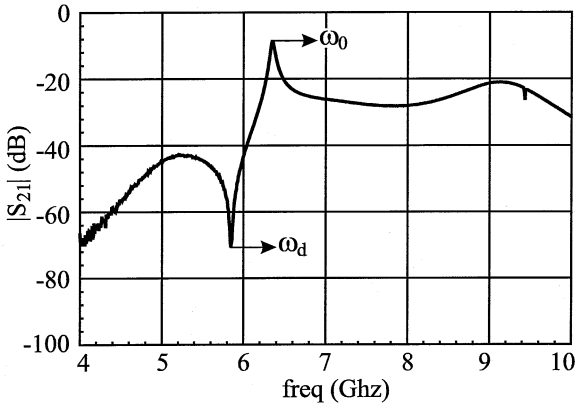

Fig. 4. A typical plot of the $|S_{21}|$ measured using the experimental setup of Fig. 3. An EC-SRR was used in this particular experiment. EC-SRR dimensions are $r_{\text{ext}} = 2.6$ mm, $c = 0.6$ mm, $d = 0.2$ mm. Substrate of thickness $t = 0.49$ mm and permittivity $\varepsilon = 2.43\,\varepsilon_0$, with metallizations made of copper with thickness $h = 35$ μm and conductivity $\sigma = 6 \times 10^7$S/m.

$$\mathbf{m}_{\text{eq}} = -\frac{4R^3}{3\mu_0}\mathbf{B}_0 \tag{18}$$

where R is the radius of the aperture and $\mathbf{B}_0$ the magnetic field in the waveguide if the aperture was not present. Since the SRR is paramagnetic below resonance [see (8)], there must be certain

frequency $\omega_{\rm d} < \omega_0$ at which the induced dipole in the SRR cancels out the equivalent dipole of the aperture without the SRR (18). At this frequency, the radiation from the SRR-loaded aperture toward the output will be substantially reduced, thus originating the *dip* observed in the $|S_{21}|$ plot. By equating the magnitudes of the magnetic dipoles in (2), (5), and (18), α_0 in (8) can be determined. It should be noted that the external magnetic flux density at the center of the aperture is half the external magnetic flux density that would be in the waveguide if the aperture was not present [26]. Taking this fact into account, the final result for α_0 is given by

$$\alpha_0 = \frac{8R^3}{3\mu_0}\left(\frac{\omega_0^2}{\omega_{\rm d}^2} - 1\right) \tag{19}$$

thus, providing a method to obtain the experimental value of α_0 from the measurement of the resonance frequency ω_0 and the *dip* frequency $\omega_{\rm d}$.

Finally it should be mentioned that an accurate measurement of ω_0 and α_0 by means of the above procedure requires the aperture diameter to be chosen in such a way that the resonance frequency is not substantially affected by the SRR-aperture coupling. Measurements of the resonance frequency, made by placing the SRR in the waveguide without the metallic screen, have shown that both measurements agree with an error less than 1% for the chosen diameter of the screen (6 mm) and for the particle sizes considered in the experiments (see Section IV).

IV. Numerical and Experimental Results

In order to verify the accuracy of the proposed theoretical model, a set of EC- and BC-SRRs were printed on a commercial metallized substrate with dielectric constant $\varepsilon = 2.43\varepsilon_0$, thickness $t = 0.49$ mm and copper metallizations with thickness $h = 35$ μm and conductivity $\sigma = 6 \times 10^7$ S/m. The resonance frequency and α_0 were measured using the technique reported in Section III for each SRR. The theoretical results were computed using the model reported in Section II. The computed theoretical results and the measured results are shown in Fig. 5(a) to (d).

Different values of the external radius $r_{\rm ext}$ and strip width c of the SRRs were considered. An acceptable agreement can be observed between the theoretical and experimental results. This agreement shows that the proposed model, despite of its simplicity, can account for the description of the main EC- and BC-SRRs characteristics. Disagreements mainly occur for the highest values of $c/r_{\rm ext}$. This fact is somewhat expected since the description of the ring response to an external excitation in terms of the ring inductance is less accurate for these cases. The behavior of the resonance frequency and α_0 with respect to the external radius is similar for both the EC- and the BC-SRR. However, the dependence with the strip width c is quite different. The BC-SRR seems to be almost insensitive to c whereas the resonance frequency of the EC-SRR increases with c. This fact can be explained considering that the p.u.l. capacitance and the inductance have opposite variations with c for the BC-SRR. However, the p.u.l. capacitance is rather insensitive to c for the EC-SRR.

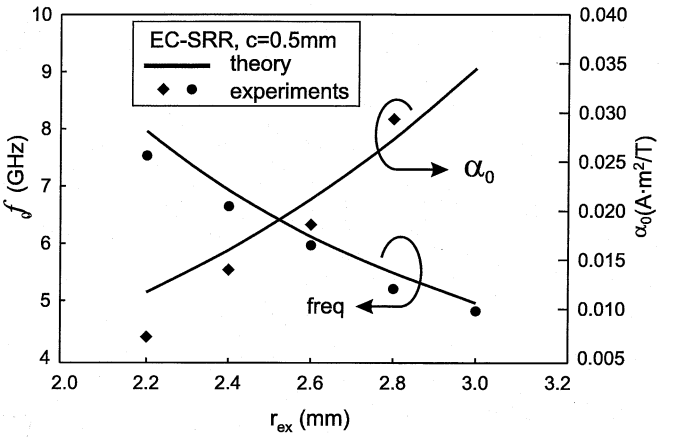

(a)

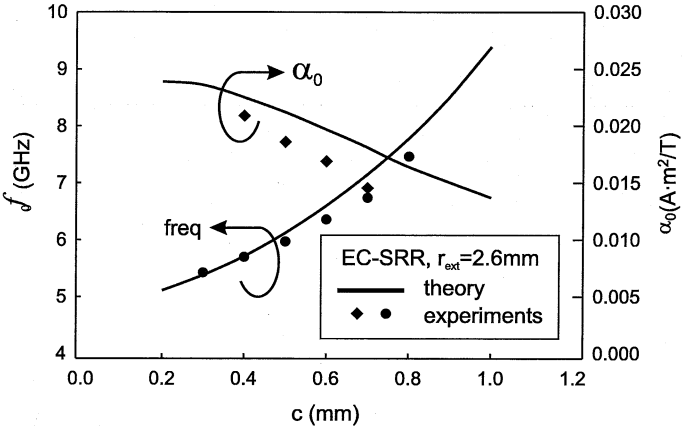

(b)

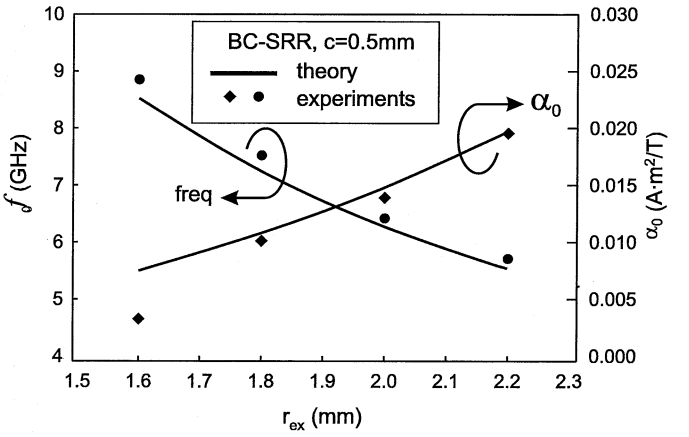

(c)

Fig. 5. Measured (dots and diamonds) and computed (solid lines) values for the resonance frequency, $f_0 = \omega_0/2\pi$, and α_0 for some EC-SRR and BC-SRR printed on a dielectric substrate with the same specifications as in Fig. 4.: $t = 0.49$ mm, $d = 0.2$ mm (for EC-SRR), $\varepsilon = 2.43\,\varepsilon_0$, with metallizations made of copper with a thickness $h = 35\mu$m and conductivity $\sigma = 6 \times 10^7$ S/m. The remaining EC-SRR and BC-SRR dimensions are given in each plot.

From the standpoint of metamaterials design, the most important parameter characterizing the SRRs is possibly the resonance frequency. This parameter gives the electrical size of the particle within the region of interest, which is the main limitation for the accuracy of the continuous-medium description of the metamaterial. The SRRs analyzed in Fig. 5(a) to (d) have an

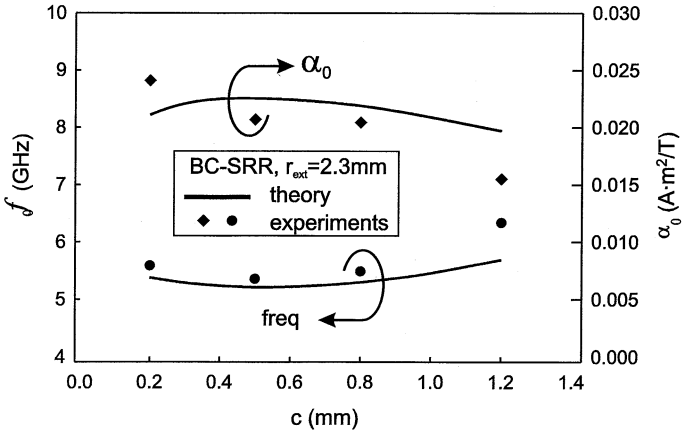

(d)

Fig. 5. (*Continued.*) Measured (dots and diamonds) and computed (solid lines) values for the resonance frequency, $f_0 = \omega_0/2\pi$, and α_0 for some EC-SRR and BC-SRR printed on a dielectric substrate with the same specifications as in Fig. 4.: $t = 0.49$ mm, $d = 0.2$ mm (for EC-SRR), $\varepsilon = 2.43\,\varepsilon_0$, with metallizations made of copper with a thickness $h = 35\ \mu$m and conductivity $\sigma = 6 \times 10^7$ S/m. The remaining EC-SRR and BC-SRR dimensions are given in each plot.

electrical size of approximately a tenth of the free-space wavelength at resonance. These values are of the same order than those reported in previous designs [6]–[9], all of them being close to the limit of applicability of the continuous-medium approach. Therefore, it is very convenient to explore the feasibility of designing SRRs with smaller electrical sizes at resonance. Assuming that the total size of the SRR remains approximately constant ($r_0 \approx \text{cte}$), (1) says that ω_0 is governed by two parameters: the total inductance L and the p.u.l. capacitance C_{pul}. Of these two quantities, the p.u.l. capacitance is more easily tunable. Changes in C_{pul} for the BC-SRR can be achieved by varying the strip width c the substrate thickness t and the dielectric constant of the substrate, ε. However, Fig. 5(d) shows that variations of C_{pul} with c are cancelled out by the associated variations of L. Therefore, there remain two main parameters for tuning: t and ε. For the EC-SRR, C_{pul} is mainly governed by the rings spacing, d, and the permittivity, ε; two parameters that do not affect L. Fig. 6(a) and (b) shows the variation of the resonance frequency and the normalized electrical size (defined as $2r_{\text{ext}}/\lambda_0$, with λ_0 being the free space wavelength at resonance) for the EC-SRR and the BC-SRR with respect to the above parameters. In Fig. 6(a) the tuning parameter is the spacing between the rings (with the substrate thickness being constant, $t = 0.4$ mm) whereas the tuning parameter in Fig. 6(b) is the substrate thickness. It can be seen that much smaller electrical sizes can be achieved using BC-SRRs instead of EC-SRRs: a particle diameter of about $\lambda_0/25$ can be obtained employing BC-SRRs printed on a commercial substrate of $\epsilon = 10\epsilon_0$ of approximately 100 μm at 10 GHz. Even smaller electrical sizes could be achieved with thinner substrates (such as oxide layers) and/or higher dielectric permittivity substrates (as ferroelectric substrates, for instance). Conversely, the electrical size of the EC-SRRs remains almost constant for small values of the spacing between the rings. Moreover, very intense electric fields should appear at the ring edges in EC-SRRs with very small spacing, which may cause high losses and/or dielectric breakdown. Since the electric field distribution is smoother in BC-SRRs, these effects are expected to be less important for this particle.

In the following, the proposed local field theory is applied to the computation of the dispersion curves of some NMPMs and LHMs. Thus, the NMPM and the LHM analyzed in [6] are newly analyzed using our model in Fig. 7. For comparison purposes, the results obtained using the commercial electromagnetic solver MAFIA reported in [6] are also shown. Notice that there is a mismatch between the frequency passbands for the LHM and the NMPM that appears both in numerical calculations and experiments. The experimental values for the LHM passband $\Delta\omega_{\text{exp}}$ and the above mismatch $\delta\omega_{\text{exp}}$ extracted from [6, Fig. 3], are equally shown in the figure. (As is explained in [20], the $\delta\omega_{\text{exp}}$ mismatch is closely related to the cross polarization effects appearing in the EC-SRR.) This plot illustrates the accuracy of the proposed simple theory: our results fr the left-handed passband appear closer to the experiments than those obtained in [6] by using a commercial full-wave solver.

As was mentioned, the use of BC-SRRs for building up metamaterials allows for a significan reduction in the electrical size of the unit cell. This fact will be illustrated in the following. The dispersion characteristic of an isotropic 2-D LHM (see the inset in the figure) made using small-size BC-SRRs is shown in Fig. 8. The reported LHM is designed following the theory reported in [9]. In this design, the artificial plasma is simulated by an array of parallel metallic plates [1] although for practical simulations only a pair of plates is needed. This array simulates a lossless plasma for wave propagation and electric field polarization both parallel to the plates [1]. For this wave polarization, the effective dielectric susceptibility of the artificial plasma is given by (17). The discrete NMPM is made by placing BC-SRRs symmetrically between the plates. Since the BC-SRRs response is isotropic for external magnetization perpendicular to the BC-SRR plane, the electromagnetic response of the device is then isotropic in this plane and for this specific polarization of the incident wave [9]. As it was theoretically and experimentally shown in [9], the proposed device behaves as an LHM (for the appropriate wave polarization) in certain frequency band that lies above the resonance frequency of the BC-SRR. This fact has been advantageously used, along with the data provided in Fig. 6(b), to design a LHM whose unit cell has a very small electrical size. Thus, the results shown in Fig. 8 have been computed for BC-SRRs with external radius $r_{\text{ext}} = 0.6$ mm and ring width $c = 0.2$ mm printed on a dielectric substrate of $\varepsilon = 10\varepsilon_0$ and thickness $t = 0.01$ mm. For the chosen lattice parameter $a = 1.5$ mm the device shows an LHM passband around 3.3 GHz. Notice that within this passband the normalized electrical size of the unit cell (a/λ_0, λ_0 is the free-space wavelength) is approximately 0.015. This electrical size is one order of magnitude smaller than the previously reported ones [6], [7], [9]. This fact proves the usefulness of the proposed BC-SRRs for designing discrete LHM with small size unit cells; namely, discrete LHM that can be accurately described by a continuous medium approach.

V. Conclusion

A self-consistent quasi-analytical model for the polarizabilities of EC-SRR and BC-SRR has been presented. The accuracy

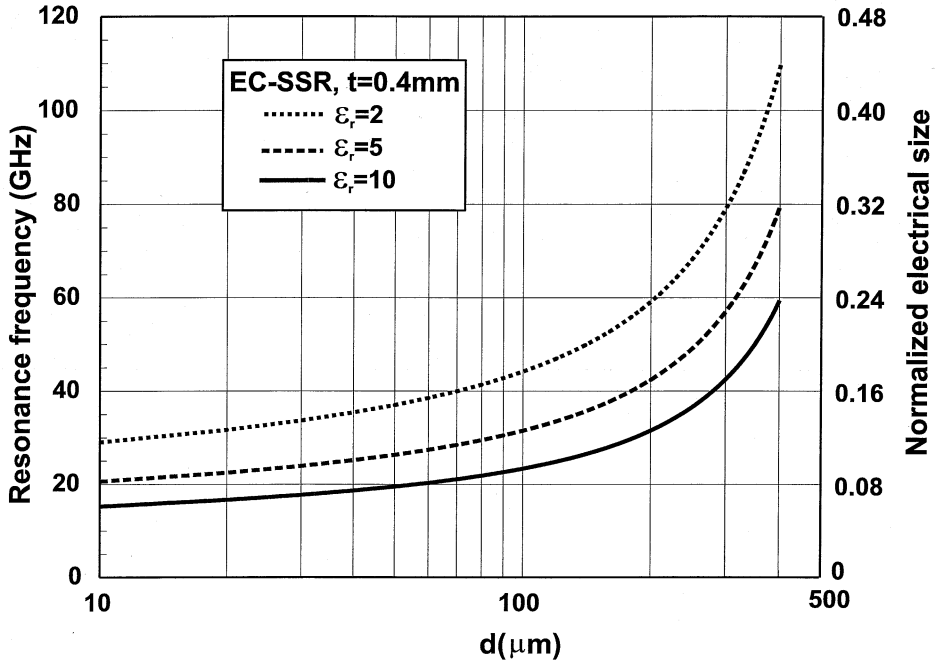

(a)

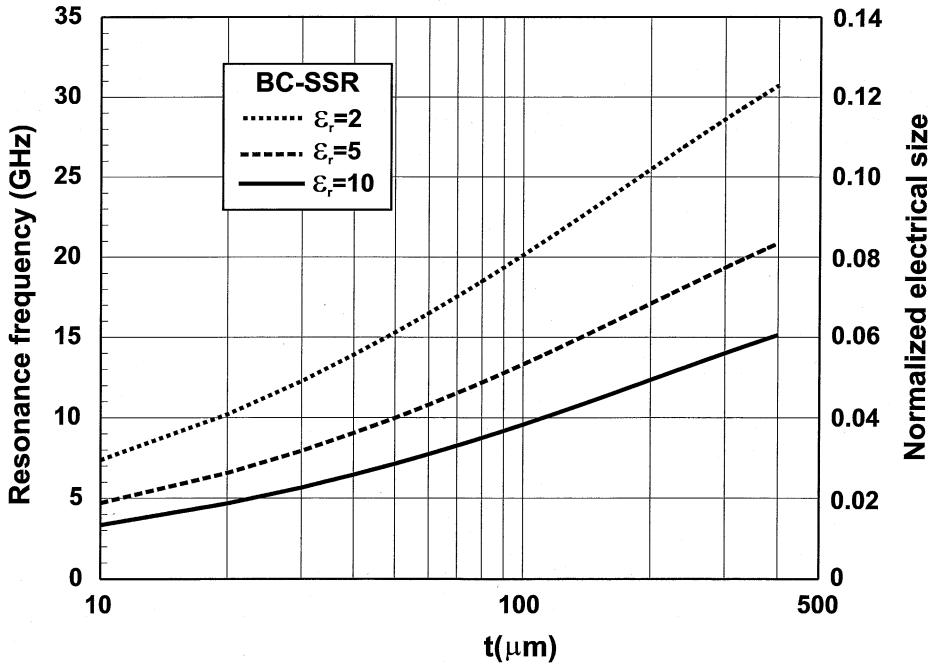

(b)

Fig. 6. Resonance frequency and normalized electrical size for several (a) EC-SRR and (b) BC-SRR with the same external radius $r_{\rm ext} = 0.6$ mm and ring width $c = 0.2$ mm, printed on several substrates.

of this model has been validated by experiments. In particular, an experimental setup for measuring the resonance frequency and the magnetic polarizabilities of both types of SRRs has been proposed and realized. Since the SRR polarizabilities have not been previously measured, the proposed experimental method for the characterization of SRRs is one of the most relevant contributions of this work. The obtained experimental results have been satisfactorily compared with theoretical results computed following the proposed model.

Starting from the proposed model, and making use of the well-known Lorentz theory, a local field model for SRR-based NMPM has been developed. This model is also useful for computing the dispersion characteristics of LHM made by a superposition of the aforementioned SRR-based NMPM and wire- or parallel plate-made artificial plasmas. This local field model has been tested by computing the dispersion characteristics of some previously reported LHM, which show an acceptable agreement with previously reported theoretical and experimental data. The simplicity and small numerical effort involved in the proposed local field model makes this approach to be a useful and efficient alternative for the analysis and design of discrete NMPM and LHM. As an additional advantage of this approach, it may

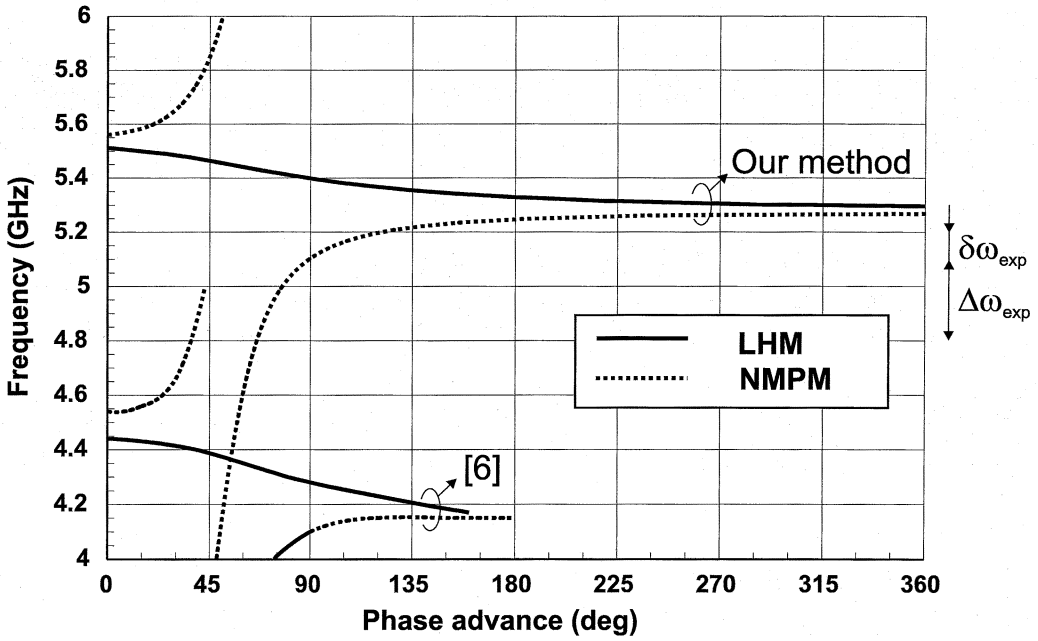

Fig. 7. Dispersion curves for the LHM and NMPM media reported in [6]. The results reported in [6, Fig. 2(a) and (c)] are also shown for comparison purposes. The experimental values for the LHM passband, $\Delta\omega_{\rm exp}$, and for the mismatch between the LHM and the NMPM passbands, $\delta\omega_{\rm exp}$, obtained from [6, Fig. 3] are indicated in the right axis of the figure.

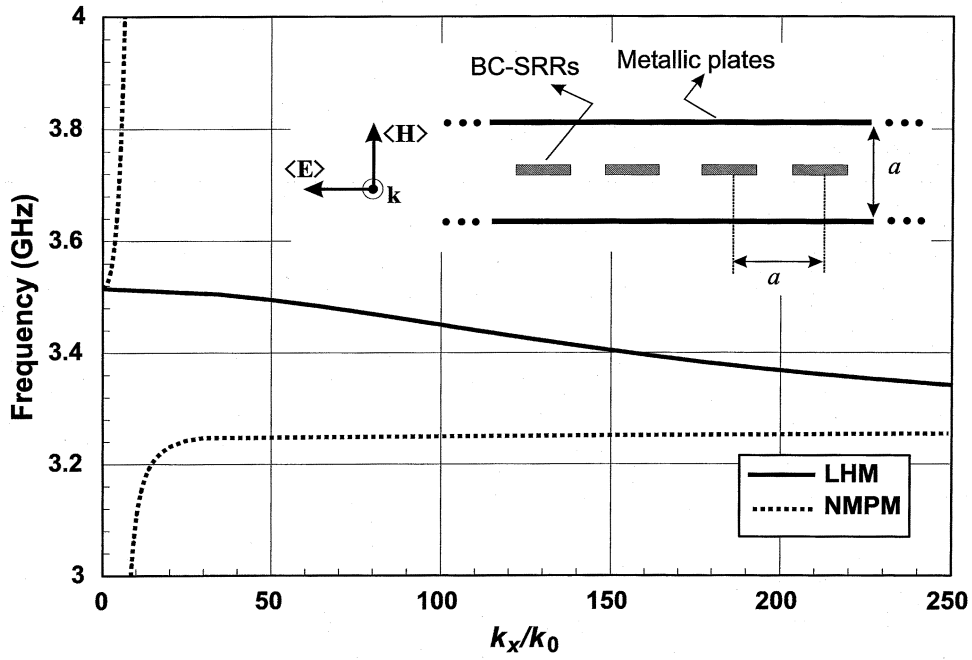

Fig. 8. Dispersion curves for the 2-D isotropic LHM and NMPM shown in the inset. The lattice parameter is $a = 1.5$ mm and the BC-SRR dimensions are $r_{\rm ext} = 0.6$ mm and $c = 0.2$ mm. The BC-SRR are printed on a substrate of thickness $t = 0.01$ mm and $\varepsilon = 10\varepsilon_0$.

provide further physical insight on some characteristics of these metamaterials (for instance, in the analysis of bianisotropic effects in EC-SRR made LHM).

Once the accuracy of the proposed model has been checked, a comparative analysis of both EC- and BC-SRR has been carried out. It has been found that this latter particle has two main advantages over the EC-SRR: isotropy in the plane of the structure (for normally incident magnetic field) and a potentially much smaller electrical size. The first property can be useful in designing isotropic LHM and NMPM for experimentation in negative refractive index and related phenomena. The second property is useful for designing discrete metamaterials with electrically small unit cells. Since the suitability of the continuous-medium approach critically depends on the electrical size of the unit cell, this property may result in substantial improvements in the design of new continuous-like metamaterials.

APPENDIX
COMPUTATION OF THE TOTAL INDUCTANCE L

Let us assume a current I on the ring of Fig. 2. Since there is no field and/or current dependence on the azimuthal coordinate ϕ the magnetostatic energy can be computed as

$$U_M = \pi \int_0^\infty r A_\phi J_{s,\phi} dr \tag{20}$$

where A_ϕ is the azimuthal component of the vector magnetic potential. Integrating by parts and using that $B_z = r^{-1}\partial_r(rA_\phi)$, where B_z is the z component of the magnetostatic field and ∂_α the partial derivative with respect to α, it is found that

$$U_M = \pi \int_0^\infty r B_z I(r) dr \tag{21}$$

where $I(r)$ is defined by (14) and (15). Since the currents are restricted to the $z = 0$ plane, B_z can be derived from a scalar magnetic potential $\psi(r,z)$: $B_z = -\mu_0 \partial_z \psi$. This scalar magnetic potential must satisfy Laplace's equation $\partial_z^2 + r^{-1}\partial_r(r\partial_r\psi) = 0$, subjected to the following boundary conditions: $\partial_z\psi(r,0^+) = \partial_z\psi(r,0^-)$; $I(r) = \psi(r,0^+) - \psi(r,0^-)$ and $\psi(\infty,z) \equiv \psi(r,\infty) = 0$. Taking the Fourier-Bessel transform, which is defined as

$$\widetilde{F}(k) = \int_0^\infty r J_0(kr) F(r) dr \tag{22}$$

the above problem is analytically solved for $\widetilde{\psi}(k,z)$, which is found to be

$$\widetilde{\psi}(k,z) = \pm \frac{1}{2} \widetilde{I}(k) e^{\mp kz} \tag{23}$$

where the upper (lower) sign stands for $z > 0$ ($z < 0$). Equation (13) is obtained after introducing $B_z = -\mu_0 \partial_z \psi$ into (21), using (22) and (23) and making use of the Parseval theorem and the relation $L = 2U_M/I^2$.

Finally, if $I(r)$ is assumed to be given by (14)–(15), after some algebraic manipulations, the ring inductance can be obtained as the following integral:

$$\frac{L}{\mu_0} = \frac{\pi^3}{4c^2} \int_0^\infty \frac{1}{k^2} \left[b\mathcal{B}(kb) - a\mathcal{B}(ka) \right]^2 dk \tag{24}$$

where $a = r_0 - c/2$, $b = r_0 + c/2$, and function $\mathcal{B}(x)$ is defined as

$$\mathcal{B}(x) = S_0(x)J_1(x) - S_1(x)J_0(x) \tag{25}$$

with S_n and J_n being the nth order Struve and Bessel functions, respectively.

REFERENCES

[1] W. Rotman, "Plasma simulation by artificial dielectrics and parallel-plate media," *IRE Trans. Antennas Propagat.*, vol. AP-10, pp. 82–95, Jan. 1962.

[2] J. B. Pendry, A. J. Holden, W. J. Stewart, and I. Youngs, "Extremely low frequency plasmons in metallic mesostructures," *Phys. Rev. Lett.*, vol. 76, pp. 4773–4776, June 1996.

[3] J. M. Pitarke, F. J. García Vidal, and J. B. Pendry, "Effective electronic response of a system of metallic cilinders," *Phys. Rev. B*, vol. 57, pp. 15 261–15 266, June 1998.

[4] J. B. Pendry, A. J. Holden, D. J. Ribbins, and W. J. Stewart, "Magnetism from conductors and enhanced nonlinear phenomena," *IEEE Trans. Microwave Theory Tech.*, vol. 47, pp. 2075–2084, Nov. 1999.

[5] V. G. Veselago, "Electrodynamics of substances with simultaneously negative electrical and magnetic properties," *Sov. Phyis. USPEKHI*, vol. 10, pp. 509–517, 1968.

[6] D. R. Smith, W. J. Padilla, D. C. Vier, S. C. Nemat-Nasser, and S. Schultz, "Composite medium with simultaneously negative permeability and permittivity," *Phys. Rev. Lett.*, vol. 84, pp. 4184–4187, May 2000.

[7] R. A. Shelby, D. R. Smith, S. C. Nemat-Nasser, and S. Schultz, "Microwave transmission through a two-dimensional, isotropic, left-handed metamaterial," *Appl. Phys. Lett.*, vol. 78, pp. 489–491, Jan. 2001.

[8] R. Marqués, J. Martel, F. Mesa, and F. Medina, "Left-handed media simulation and trnsmission of EM waves in subwavelength split-ring-resonator-loaded metallic waveguides," *Phys. Rev. Lett.*, vol. 89, pp. 13 901(1)–13 901(4), Oct. 2002.

[9] ——, "A new 2-D isotropic left-handed metamaterial design: Theory and experiment," *Microwave Opt. Tech. Lett.*, vol. 36, pp. 405–408, Dec. 2002.

[10] T. Weiland, R. Schumann, R. B. Greegor, C. G. Parazzoli, A. M. Vetter, D. R. Smith, D. C. Vier, and S. Schultz, "Ab initio numerical simulations of left-handed metamaterials: Comparison of calculations and experiments," *J. Appl. Phys.*, vol. 90, pp. 5419–5424, Nov. 2001.

[11] P. Markos and C. M. Soukoulis, "Numerical studies of left-handed materials and arrays of split ring resonators," *Phys. Rev. B*, vol. 65, pp. 036 622(1)–036 622(8), 2002.

[12] A. Sihvola, *Electromagnetic Mixing Formulas and Applications*. London, U.K.: IEE, 1999.

[13] R. E. Collin, *Field Theory of Guided Waves*. New York: IEEE, 1991.

[14] Y. N. Kazantsev, M. V. Kostin, G. A. Kraftmakher, V. I. Pomonarenko, and V. V. Shevshenko, "Artificial paramagnetic," *J. Commun. Tech. Electron.*, vol. 39, pp. 78–81, 1994.

[15] M. V. Kostin and V. V. Shevshenko, "Artificial magnetics based on double circular elements," in *Proc. Chiral'94, 3rd Int. Workshop on Chiral, Bi-Isotropic and Bi-Anisotropic Media*, F. Mariotte and J.-P. Parneix, Eds., Perigueux, France, May 1994, pp. 50–56.

[16] A. J. Bahr and K. R. Clausing, "An approximate model for artificial chiral material," *IEEE Trans. Microwave Theory Tech.*, vol. 42, pp. 1592–1599, Dec. 1994.

[17] F. Mariotte, S. A. Tretyakov, and B. Sauviac, "Isotropic chiral composite modeling: Comparison between analytical, numerical, and experimental results," *Microwave Opt. Tech. Lett.*, vol. 7, pp. 861–864, Dec. 1994.

[18] S. A. Tretyakov, F. Mariotte, C. R. Simovski, T. G. Kharina, and J.-P. Heliot, *Analytical Antenna Model for Chiral Scatterers: Camparison with Numerical and Experimantal Data*, vol. 44, pp. 1006–1014, July 1996.

[19] M. M. I. Saadoun and N. Engheta, "A reciprocal phase shifter using a novel pseudochiral or Ω medium," *Microwave Opt. Tech. Lett.*, vol. 5, pp. 184–188, Apr. 1992.

[20] R. Marqués, F. Medina, and R. Rafii-El-Idrissi, "Role of bianisotropy in negative permeability and left-handed metamaterials," *Phys. Rev. B*, vol. 65, pp. 144 440(1)–144 440(6), 2002.

[21] I. Bahl and P. Bhartia, *Microwave Solid State Circuit Design*. New York: Wiley, 1988.

[22] F. Tefiku and E. Yamashita, "Capacitance characterization method for thick-conductor multiple planar ring structures on multiple substrate layers," *IEEE Trans. Microwave Theory Tech.*, vol. 40, pp. 1894–1902, Oct. 1992.

[23] D. R. Smith, W. J. Padilla, D. Vier, R. Shelby, S. Nemat-Nasser, N. Kroll, and S. Schultz, "Left-handed metamaterials," in *Photonic Crystals and Light Localization in the 21st Century*, C. M. Soukoulis, Ed. Dordrecht, The Netherlands: Kluwer, 2001.

[24] P. Gay-Balmaz and O. J. F. Martin, "Electromagnetic resonances in individual and coupled split-ring resonators," *J. Appl. Phys.*, vol. 92, pp. 2929–2936, Sept. 2002.

[25] H. A. Bethe, "Theory of diffraction by small holes," *Phys. Rev.*, vol. 66, pp. 163–182, Oct. 1944.

[26] D. M. Pozar, *Microwave Engineering*. New York: Wiley , 1998.

Ricardo Marqués (M'95) was born in San Fernando, Cádiz, Spain. He received the Ph.D. degree from the Universidad de Sevilla, Spain, in 1987.

He is currently an Associate Professor with the Departamento de Electrónica y Electromagnetismo, Universidad de Sevilla. His main scientific activity has been for many years in the computer-aided design of planar transmission lines and circuits at microwave frequencies, with emphasis in the influence and applications of complex media, such as anisotropic dielectrics, magnetized ferrites and plasmas, as well as bi(iso/aniso)tropic materials. He is also interested in the electromagnetic analysis and characterization of discrete metamaterials, including bianisotropic and LHM.

Prof. Marques has been and/or is a reviewer for the IEEE TRANSACTIONS ON MICROWAVE THEORY AND TECHNIQUES, the IEEE TRANSACTIONS ON ANTENNAS AND PROPAGATION, and other scientific and technical journals and conferences.

Francisco Mesa (M'02) was born in Cádiz, Spain, on April 1965. He received the Licenciado degree in June 1989 and the Doctor degree in December 1991, both in physics, from the University of Seville, Spain.

He is currently an Associate Professor with the Department of Applied Physic 1, University of Seville. His research interest focus on electromagnetic propagation/radiation in planar structures with general anisotropic materials and metamaterials.

Jesús Martel was born in Seville, Spain, in 1966. He received the Licenciado and Doctor degrees in physics from the University of Seville, in 1989 and 1996, respectively.

Since 1992, he has been with the Department of Applied Physics II, University of Seville, where, in 2000, he became an Associate Professor. His current research interest is focused on the numerical analysis of planar transmission lines, the modeling of planar microstrip discontinuities, the design of passive microwave circuits, microwave measurements, and artificial media.

Francisco Medina (M'90–SM'01) was born in Puerto Real, Cádiz, Spain, in November 1960. He received the Licenciado (with honors) and Doctor degrees from the University of Seville, Seville, Spain, in 1983 and 1987, respectively, both in physics.

From 1986 to 1987, he spent the academic year at the Laboratoire de Microondes de l'ENSEEIHT, Toulouse, France, thanks to a scholarship of the Ministerio de Educación y Ciencia, Spain, and Ministère de la Recherche et la Technologie, France. From 1985 to 1989, he was an Assistant Professor with the Department of Electronics and Electromagnetism, University of Seville, and since 1990, he has been an Associate Professor of electromagnetism. He is also currently Head of the Microwaves Group, University of Seville. His research interest includes analytical and numerical methods for guidance, resonant and radiating structures, passive planar circuits, periodic structures, and the influence of anisotropic materials on such systems. He is also interested in artificial media modeling and design.

Dr. Medina was a member of the Technical Programme Committees (TPC) of the 23rd European Microwave Conference, Madrid, Spain, 1993, the ISRAMT'99, Málaga, Spain, 1999, and member of the TPC of the Microwaves Symposium 2000, Tetouan, Morocco, 2000. He was co-organizer of the workshop *New Trends on Computational Electromagnetics for Open and Boxed Microwave Structures*, Madrid, Spain, 1993. He is on the editorial board of the IEEE TRANSACTIONS ON MICROWAVE THEORY AND TECHNIQUES and acts as reviewer for other IEEE, Institution of Electrical Engineers (IEE), U.K., and American Physics Association journals. He was the recipient of two scholarships.